Redox Biology 32 (2020) 101500

Contents lists available at ScienceDirect

Redox Biology

journal homepage: www.elsevier.com/locate/redox

Research Paper

# Breaking the vicious loop between inflammation, oxidative stress and coagulation, a novel anti-thrombus insight of nattokinase by inhibiting LPS-induced inflammation and oxidative stress

Hao Wu[a], Ying Wang[a], Yupeng Zhang[a], Feng Xu[a], Jiepeng Chen[b], Lili Duan[b], Tingting Zhang[a], Jian Wang[c,**], Fengjiao Zhang[a,*]

[a] Wuya College of Innovation, Shenyang Pharmaceutical University, Shenyang, Liaoning, 110016, China
[b] Sungen Biotech Co., Ltd, Shantou, 515000, PR China
[c] Key Laboratory of Structure-Based Drug Design & Discovery, Ministry of Education, Shenyang Pharmaceutical University, Shenyang, Liaoning, 110016, China

ARTICLE INFO

*Keywords:*
Nattokinase
TRL4
NOX2
Inflammation
Oxidative stress
Thrombus

ABSTRACT

Thrombosis is a principle cause of cardiovascular disease, the leading cause of morbidity and mortality worldwide; however, the conventional anti-thrombotic approach often leads to bleeding complications despite extensive clinical management and monitoring. In view of the intense crosstalk between inflammation and coagulation, plus the contributing role of ROS to both inflammation and coagulation, it is highly desirable to develop safer anti-thrombotic agent with preserved anti-inflammatory and anti-oxidative stress activities. Nattokinase (NK) possesses many beneficial effects on cardiovascular system due to its strong thrombolytic and anticoagulant activities. Herein, we demonstrated that NK not only effectively prevented xylene-induced ear oedema in mice, but also remarkably protected against LPS-induced acute kidney injury in mice through restraining inflammation and oxidative stress, a central player in the initiation and progression of inflammation. Fascinatingly, in line with our in vivo data, NK elicited prominent anti-inflammatory activity in RAW264.7 macrophages via suppressing the LPS-induced TLR4 and NOX2 activation, thereby repressing the corresponding ROS production, MAPKs activation, and NF-κB translocation from the cytoplasm to the nucleus, where it mediates the expression of pro-inflammatory mediators, such as TNF-α, IL-6, NO, and PAI-1 in activated macrophage cells. In particular, consistent with the macrophage studies, NK markedly inhibited serum PAI-1 levels induced by LPS, thereby blocking the deposition of fibrin in the glomeruli of endotoxin-treated animals. In summary, we extended the anti-thrombus mechanism of NK by demonstrating the anti-inflammatory and anti-oxidative stress effects of NK in ameliorating LPS-activated macrophage signaling and protecting against LPS-stimulated AKI as well as glomeruler thrombus in mice, opening a comprehensive anti-thrombus strategy by breaking the vicious cycle between inflammation, oxidative stress and thrombosis.

## 1. Introduction

In spite of major scientific improvements, cardiovascular diseases remain the leading cause of morbidity and mortality worldwide. Indeed, thrombosis is the principle cause of the three major cardiovascular disorders: heart attacks, stroke and venous thromboembolism. Administration of thrombolytic drugs (e.g., tPA) to disintegrate fibrin clots is the most common and preferred treatment for thrombotic events; however, this approach often leads to severe bleeding complications despite the extensive clinical management [1]. Thus, a formidable challenge remains in identifying anti-thrombotic approach that are effective and can be safely used in clinic.

Historically, thrombus resolution was believed to be achieved by thrombolysis, however, increasing evidence points to an extensive crosstalk between the systems of inflammation and coagulation, whereby inflammation, the silent killer, leads to activation of coagulation that stimulates thrombosis, and in turn, thrombosis considerably promotes inflammation, which occurs at the levels of platelet activation, fibrin formation, and physiological anticoagulant pathways [2–4]. For example, during sepsis, inflammatory mediators derived from pathogens and activated immune cells stimulate systemic inflammatory response that gives rise to a systemic coagulation activation. The

* Corresponding author.
** Corresponding author.
*E-mail addresses:* jianwang@syphu.edu.cn (J. Wang), zhangfengjiao@syphu.edu.cn (F. Zhang).

https://doi.org/10.1016/j.redox.2020.101500
Received 13 December 2019; Received in revised form 1 March 2020; Accepted 7 March 2020
Available online 11 March 2020

ultimate extent of organ injury is not only dependent on the primary insult by bacterial LPS, but also by the extent of the ensuing vascular thrombo-inflammatory response. When severe, thrombo-inflammation can extend systemically and damage remote organs, particularly kidneys leading to AKI and even death [5]. However, rather than this being a one-way process, both systems closely interact, whereby coagulation factors (such as thrombin) or anticoagulant proteins may activate specific cell receptors on mononuclear cells or endothelial cells, which may promote cytokine production, forming an essential amplification loop. In particular, oxidative stress has been highlighted in the initiation and progression of both inflammation and coagulation [6–8]. In this setting, it is reasonable to propose that simultaneous modulation of both coagulation, oxidative stress and inflammation, rather than specific therapies aimed at one of these systems, will be more successful for managing thrombotic disorders. Therefore, it is highly desirable to develop safer anti-thrombotic agent with preserved anti-inflammatory and anti-oxidative stress function.

NK is a serine protease from the traditional Japanese food Natto, and possesses many cardiovascular beneficial effects due to its thrombolytic and anticoagulant activities [9,10]. A clinical trial demonstrated that oral consumption of NK was not associated with any adverse effects [11]. In line with this notion, we reported recently that it showed no genotoxicity, and the maximum daily tolerant dose of NK in mice is 1000 times more compared to the recommended daily dose for human [12]. Yet, it is not clear whether NK holds promise as an anti-thrombus agent with anti-inflammation and/or anti-oxidative stress capacity that would prevent accelerated thrombosis formation. In this study, we offered the proof that in addition to its thrombolytic and anticoagulant activities, NK elicited anti-inflammatory and anti-oxidative stress activities by inhibiting LPS-mediated TLR-4 and NOX2 signaling in macrophages and protected against LPS-stimulated AKI as well as glomeruli thrombus in mice, a novel anti-thrombus insight of NK via breaking the link between inflammation, oxidative stress and thrombosis.

## 2. Materials & methods

### 2.1. Chemicals and reagents

Nattokinase was from Sungen Biotech Co., Ltd. Lipopolysaccharides (LPS), 2′,7′-Dichlorodihydrofluorescein diacetate (DCFH2-DA), and Hoechst 33258 were all obtained from Sigma-Aldrich (St. Louis, MO, USA). Duefflbecco's modified eagle medium (DMEM) and fetal bovine serum (FBS) were obtained from Life Technologies/Gibco Laboratories (Grand Island, NY, USA). Antibodies for p-IκB-α (AF2002), P65 (AF0874), P38 (AF6455), ERK (AF0155), TRAF6 (AF5376), NRF2 (AF0639), p-AKT (AF0016), AKT (AF6261), and β-actin (T0022) were obtained from Affinity bioscience (Cincinnati, OH, USA). p-JNK (ab130943), p-ERK (abs130614), p-P38 (abs131122), and JNK (abs131832) antibodies were purchased from Absin Bioscience Co., Ltd. (Shanghai, China). Antibodies for IκB-α (sc-1643) and P47 (SC-365215) were obtained from Santa Cruz Biotechnology, INC. (Bergheimer Heidelberg Germany). And Toll-like receptor 4 (TLR4, GB11519) as well as NOX-2/gp91 (GB11391) antibodies were obtained from Servicebio Co., Ltd. (Wuhan, China). The Fibrinogen Alpha chain antibody was purchased from Cloud-Clone Corp. And the Goat anti-rabbit IgG (H + L) HRP (S0001) and goat anti-mouse IgG (H + L) HRP (S0002) were obtain from Affinity Science (Cincinnati, OH, USA).

### 2.2. Animals

Both 6-week-old Kunming mice (male, weighting 18–22 g) and 6-week-old rats (male, weighting 180–220 g) were obtained from the Experimental Animal Center of Shenyang Pharmaceutical University (Shenyang, China) and maintained under standard housing conditions in a 12 L: 12 D light/dark cycle with free access to food and water. Animal experiments were designed in accordance with the guidelines of the animal facility at Shenyang Pharmaceutical University and approved by the institutional ethics committee, and were conducted to minimize the number of animals used and the suffering caused by the procedures used in this study. All the experiments and procedures were carried out in accordance with the National Institutes of Health guide for the care and use of Laboratory animals.

### 2.3. Cell culture and isolation of rat peritoneal macrophages

The murine macrophage (RAW264.7) cell line was obtained from the Cell Bank of the Chinese Academy of Sciences (Shanghai, China). Cells were cultured in DMEM supplemented with 10% FBS at 37 °C under a humidified atmosphere of 5% $CO_2$ in an incubator. All experiment were done using cells of passage number 5 to 20.

Rat resident peritoneal macrophages from 6-week-old male rats (obtained from the Experimental Animal Center of Shenyang Pharmaceutical University) were prepared as described previously [13]. In brief, peritoneal cells were harvested by lavage of the peritoneal cavity with 10 mL of DMEM. These cells were incubated for 2 h and the non-adherent cells were removed by washing three times with PBS. The adherent cells were used as peritoneal macrophages. The isolated peritoneal macrophages were cultured at 37 °C in DMEM supplemented with 10% FBS in a humidified 5% $CO_2$ atmosphere.

### 2.4. Xylene-induced ear oedema of mice

Mice were segregated randomly into five groups (n = 6 per group): control group, xylene model group, and NK treated groups (3500, 7000, and 14000 FU/kg). Animals were orally administered with indicated doses of NK or $ddH_2O$ for a week before xylene application. Xylene (30 μl) was smeared to the surface of the right ears for 30 min. The left ears were untreated and served as controls. Animals were sacrificed humanely under anesthesia, and two ear punches (8 mm, i.d.) were collected and weighed. The oedema was evaluated by comparing the increase in the weight of the right ear punch with the increase in the weight of the left ear punch.

### 2.5. LPS-induced acute kidney injury (AKI) in mice

The LPS-induced AKI model was established as previously described with slight modifications [14]. To observe the effect of NK on LPS-induced AKI, mice were randomly divided into five groups (n = 10 per group): control group, (LPS + saline) group, (LPS + NK 3000 FU/kg) group, (LPS + NK 6000 FU/kg) group, and (LPS + NK 9000 FU/kg) group. The control and (LPS + saline) group were received single intraperitoneal (i.p.) injection of saline or LPS (10 mg/kg). In (LPS + NK) groups, all animals were dosed intraperitoneally with NK for 1 h before challenging with LPS for 12 h. All mice were sacrificed humanely. Blood samples were collected for measuring levels of GSH, MDA, GSH-px, TNF-α, IL-6, and PAI-1. The parts of kidney samples were taken for histopathology.

### 2.6. Histopathological evaluation

Tissues were fixed with 4% polyformaldehyde for 72 h at room temperature. After dehydration, tissues were embedded in paraffin. Tissue sections were then cut and stained with hematoxylin-eosin (H&E). Pathological changes were observed and recorded using a light microscope.

### 2.7. Enzyme-linked immunosorbent assay (ELISA)

Supernatants of cell cultures or the indicated mice serum were harvested. TNF-α, IL-6, t-PA, and PAI-1 levels were measured using ELISA according to the manufacturer's instructions (Nanjing Jiancheng Bioengineering Institute, Nanjing City, China). All measurements were

performed in triplicate.

### 2.8. Measurements of MDA and GSH levels as well as GSH-px activity

MDA and GSH levels, as well as GSH-px activities were analyzed using specific assay kits according to the manufacturers' instructions (Nanjing Jiancheng Bioengineering Institute, Nanjing City, China).

### 2.9. Nitrite determination and MTT assay

The production of NO was estimated from the accumulation of nitrite ($NO_2^-$) (a stable end product of NO metabolism) in the medium using the Griess reagent. In brief, equal amounts of culture supernatant and Griess reagent (1% sulfanilamide in 5% phosphoric acid and 0.1% α-naphthylethylenediamine dihydrochloride in distilled water) were mixed and incubated for 10 min at room temperature. The reaction was measured at 540 nm on a microplate reader (Microplate Reader Benchmark, Bio-Rad, CA, USA). For the MTT assay, MTT stock solution (5 mg/mL) was added to the cells to equal to one-tenth of the original culture volume and incubated for 4 h. The purple MTT formazan was solubilized with DMSO and measured by microplate reader (492 nm).

### 2.10. Immunofluorescence

RAW264.7 cells ($1.0 \times 10^5$ cells/well) were seeded on the glass cover slip in 24-well plates and grown for 24 h. Cells were pretreated with NK (0.3 FU/ml) for 1 h before challenging with LPS (0.1 μg/ml) for the indicated time points. Cells were washed with PBS and fixed with 4% paraformaldehyde for 30 min at room temperature. Afterwards, cells were permeabilized in PBS containing 1% BSA and 0.1% Triton X-100 for 15 min, and blocked with 1% BSA for 30 min. Then cells were incubated with specific primary antibodies overnight at 4 °C, followed by incubation with goat Anti-Rabbit lgG H&L (FITC) (ab6717, abcom) or goat Anti-Mouse lgG (H + L) Alexa Fluor 594-conjugated (S0005, Affinity) for 2 h at room temperature in the dark. After additional washes, cells were stained with Hochest mounting medium for 10 min. Fluorescence signals were analyzed through confocal microscope.

### 2.11. Western blot assay

Cells were homogenized in SDS lysis buffer containing 62.5 mM Tris-HCl (pH6.8), 2% SDS, 10% glycerol, protease and phosphatase inhibitor cocktails, and the protein concentrations were determined using the Bio-Rad protein assay kit (Bio-Rad Laboratories, Inc., Hercules, CA, USA). Samples were resolved in SDS-polyacrylamide gels and transferred to polyvinylidene difluoride (PVDF) membranes (EMD Millipore, Billerica, MA). Membranes were blocked with 5% nonfatmilk in Tris-buffered saline with 0.1% Tween 20 (TBS-T), then incubated with primary antibody overnight at 4 °C. Following washes, membranes were incubated with secondary antibody coupled with horseradish peroxidase for 1 h at room temperature. Immunoblots were developed using enhanced chemiluminescence (ECL) reaction (Pierce, Thermo Scientific, Rockwell, IL) and imaged on a ChemiDoc XRS System (BioRad, Hercules, CA). To quantify the changes in protein expression, levels were calculated as follows: (immunoreactive intensity of the target protein)/(immunoreactive intensity of internal control) using Image J software.

### 2.12. Determination of reactive oxygen species (ROS)

RAW264.7 cells were cultured in 6-well plates with a density of $1 \times 10^5$ cells/ml for 24 h. Cells were treated with various concentrations of NK before exposure to LPS (0.1 μg/ml) for 24 h. Then cells were stained with DCFH2-DA (5 μM) for 30 min at 37 °C in the dark. After washing with PBS, fluorescence signals were analyzed through confocal microscope. Fluorescence intensity was quantified using Image Pro Plus. The experiments were repeated for three times.

### 2.13. Docking of NK to TLR4

To investigate the possible molecular mechanism(s) of the decreased content of TLR4 caused by NK, in silico strategies including protein-protein docking, binding free energy calculation and molecular dynamics (MD) simulations were employed. Both TLR4 and NK structures were retrieved from protein database bank (PDB) [15] with the PDB code 5gl8 for NK and PDB code 2z64 for TLR4 [16]. Before protein-protein docking simulation, the protein structures were prepared with the protein prepare wizard in Schrodinger package and refined by restrained minimization with the force filed of OPLS-2005 [17]. Subsequently, the prepared protein structures were submitted to HawkDock online server (http://cadd.zju.edu.cn/hawkdock/) for protein-protein docking [18]. During the calculation process, TLR4 was set as receptor while NK was set as ligand, and the top 10 docking results were re-ranked according to their binding free energies calculated with molecular mechanics-generalized Born surface area (MM-GBSA) algorithm [19]. The top 10 protein complexes were analyzed with Discovery Studio 3.0 to detect the residues locating at the contacting surface which formed non-bond interactions. Furthermore, the protein complexes meeting the selection criteria of both binding mode and binding free energy were projected to MD simulation to evaluate their stability under a physiological condition with Desmond 3.8 [20]. And the protein complexes were embedded into orthorhombic boxes filled with simple point charge (SPC) model for water molecules and neutralized by adding suitable encounter ions, which were then minimized with the maximum iterations of 5000. The minimized systems were submitted to an 100 ns's MD simulations with the parameters set as default. The root-mean square deviations (RMSD) of the proteins in each system were calculated with the first frame as reference along the whole time of MD simulation. Besides, the degree of freedom, total energy and potential energy of the two systems were also calculated.

### 2.14. Wound-healing scratch assay

RAW 264.7 cells were first incubated in a 6-well plates for 24 h at 37 °C, 5% $CO_2$ and 95% humidity to form a confluent cell mono-layer. Thereafter, a wound was made in the centre of the well by drawing a p10 tip across the cell mono-layer. Cell supernatants were removed, and then the cells were washed with PBS, and treated with various concentration (0.08, 0.15 and 0.30 FU/mL) of NK, followed by LPS (0.1 μg/ml) stimulation. Cell migration into the wound was monitored by micrography, at the same location, before (time 0) and after 24-h incubation. Micrographs were acquired by inverse light microscopy with phase contrast, coupled to a computerized image capture system. The cell migration was evaluated by counting the number of cells that migrated inward after 24-h incubation, relative to time 0.

### 2.15. Neutral red phagocytosis assay

RAW 264.7 cells were seeded in a 96-well plate for 24 h before treating with NK (0.08, 0.15, 0.30 FU/ml) and challenging with LPS (0.1 μg/ml) for 24 h. Then each well was added with 0.1% neutral red solution (100 μl, dissolved in 10 mmol/L PBS) and re-incubated for 4 h. The supernatants were discarded and the cells were washed with PBS followed by adding 100 μL of cell lysis buffer [ethanol: glacial acetic acid = 1:1, (v/v)] and incubated for 2 h to extract the engulfed neutral red. The absorbance values at 540 nm were acquired using the microplate reader.

### 2.16. The LPS-induced glomerular thrombosis model in mice

The LPS-induced mice glomerular thrombosis model was

established as previously described with slight modifications [21]. To observe the effect of NK on LPS-induced glomerular thrombosis, mice were randomly divided into five groups (n = 10 per group): control group, (LPS + saline) group, (LPS + NK 3000 FU/kg) group, (LPS + NK 6000 FU/kg) group, and (LPS + NK 9000 FU/kg) group. The control and (LPS + saline) group were received single intraperitoneal (i.p.) injection of saline or LPS (0.5 mg/kg). In (LPS + NK) groups, all animals were pretreated intraperitoneally with NK for 1 h followed by challenging with LPS for 12 h. All animals were sacrificed humanely. Blood samples were collected for measuring levels of PAI-1 and t-PA. The parts of kidney samples were taken for immunohistochemical analysis.

### 2.17. Fibrin immunohistochemistry

For immunohistochemical analysis, the kidney sections were deparaffinized and treated with 3% hydrogen peroxide solution for 15 min to block endogenous peroxidase activity. Non-specific binding sites were blocked with Ultra V Block reagent followed by incubation overnight at 4 °C with anti-fibrin(ogen) IgG diluted 1:100 in PBS. After a washing step, the sections were incubated with the secondary antibody (a biotinylated anti-rabbit IgG produced in goat) which conjugated with streptavidin. The chromogenic reaction was developed by incubating the sections with 0.05% diaminobenzidine solution and 0.2% hydrogen peroxide. The progress of the reaction was monitored by light microscopy and stopped by washing the slides. Finally, the sections were counter stained with hematoxylin. The quantitative area of fibrin deposition in the glomerulus was analyzed using Image J. Six glomeruli per mouse from each group and eight mice per group were randomly and blindly selected and analyzed.

### 2.18. Statistical analysis

All values are expressed as mean ± SD. Statistical analysis was carried out using SPSS 17.0 software for Windows (SPSS Inc., Chicago, IL, USA). Student's t-test was used to compare the difference between two experimental groups, while one-way ANOVA followed by multiple comparison tests (LSD) was used to compare the differences among three or more groups. If the variance among groups was not homogeneous, Dunnett's T3 test was performed. The level of significance was considered as $p < 0.05$.

## 3. Results

### 3.1. NK effectively protected against xylene-induced ear oedema and LPS-induced AKI in mice

To investigate the anti-inflammatory potential of NK, two types of inflammation models in mice were employed. In the xylene-induced ear oedema model it was found that oral administration of NK dose-dependently reduced the ear oedema in mice (Fig. 1A), indicating that NK remarkably suppressed acute inflammation in vivo. Alternatively, LPS is among the most important factors that lead to AKI [22] due to its important role in stimulating the production of pro-inflammatory cytokines; hence the LPS-induced AKI model was subsequently employed to examine the effect of NK on systemic inflammatory response. As reflected by H&E staining, the renal tissues revealed normal kidney tubules in control animals, whereas LPS treatment resulted in atrophy of the glomerulus, destruction of tubular structures, and loss of the epithelial cells, which were remarkably alleviated by NK treatment (Fig. 1B). In line with this, NK dose-dependently reduced the LPS-induced inflammatory cytokines levels, such as TNF-α (Fig. 1C), and IL-6 (Fig. 1D). Simultaneously, it was observed that LPS challenge triggered oxidative stress as reflected by the resultant enhance in MDA levels in serum (Fig. 1E), the lipid peroxidation marker, as well as the depletion of GSH (Fig. 1F) and GSH-px levels (Fig. 1G), reflecting the key role of oxidative stress in the manifestation of LPS-induced disorders [23]. Of note, NK pretreatment not only significantly reduced the serum MDA levels (Fig. 1E), but also remarkably increased the GSH and GSH-px levels compared with those in LPS-treated animals (Fig. 1F and G). Accordingly, NK displayed effective protection against LPS-induced AKI, at least in part, through restraining inflammation and oxidative stress. Together, these data demonstrated a remarkable anti-inflammatory and anti-oxidative stress efficacy of NK.

### 3.2. NK significantly repressed LPS-induced nitric oxide (NO) release in both RAW264.7 and rat primary peritoneal macrophage cells

The in vivo anti-inflammatory and anti-oxidative stress efficacy of NK set our stage for further elucidating its underlying molecular basis in vitro. Macrophages are classically activated by pro-inflammatory stimuli like LPS, leading to a pro-inflammatory switch, and central to this switch is the expression of inducible nitric oxide synthase (iNOS), which generates large quantities of NO, contributing to the production of reactive nitrogen species [24]. In light of this, we determined to investigate the anti-inflammatory potential of NK via testing the effect of NK on LPS-induced NO release in macrophage cells. In terms of RAW264.7 cells, it was found that NK prominently suppressed LPS-stimulated NO levels in a concentration-dependent pattern (Fig. 2A). Meanwhile, as shown in Fig. 2B, NK didn't affect the cell viability of RAW264.7 macrophage. Similarly, it was observed that NK dose-dependently decreased LPS-induced NO levels in rat primary peritoneal macrophages without affecting the cell viability (Fig. 2C and D). Collectively, these findings indicated that NK suppressed LPS-induced NO release in both RAW 264.7 and rat primary peritoneal macrophages, suggesting a promising anti-inflammatory and anti-oxidative stress potential of NK in macrophage cells.

### 3.3. NK efficiently inhibited LPS-induced NF-κB activation and its downstream pro-inflammatory mediators production in RAW264.7 cells

NF-κB is a transcription factor that activates numerous genes that regulate several immune and inflammatory processes [25]. To verify the anti-inflammatory effect of NK in macrophage, the effect of NK on LPS-induced NF-κB activation in RAW 264.7 cells was further explored. Typically, NF-κB activation is mediated by phosphorylation and rapid degradation of IκB-α, followed by translocation of NF-κB to the nucleus, where it activates transcription of pro-inflammatory genes [26]. In this respect, LPS was shown to induce IκB-α phosphorylation and degradation, which were significantly inhibited by NK in a concentration-dependent pattern (Fig. 3A). Along similar lines, it was revealed that LPS stimulated the translocation of NF-κB to the nucleus (Fig. 3B), where it activated transcription of pro-inflammatory genes, and thereby led to excessive levels of pro-inflammatory cytokines, such as TNF-α (Fig. 3C) and IL-6 (Fig. 3D). Fascinatingly, NK impressively abolished the NF-κB translocation (Fig. 3B), as well as significantly reduced the excessive levels of TNF-α (Fig. 3C) and IL-6 (Fig. 3D) induced by LPS in RAW264.7 cells. Together, these data indicated that NK efficiently inhibited LPS-induced NF-κB activation and its downstream pro-inflammatory mediators production in RAW264.7 macrophages, confirming the anti-inflammatory efficacy of NK in macrophage cells. Therefore, in addition to the anti-inflammatory efficacy in vivo, NK also displayed remarkable anti-inflammatory activity in vitro.

### 3.4. NK suppressed LPS-induced ROS generation and NOX2 activation in RAW264.7 cells

In addition to pro-inflammatory mediators, oxidative stress is highlighted in the initiation and progression of inflammation [6]. Indeed, LPS rapidly induces ROS generation in macrophage cells, which plays an important role in NF-κB activation [27]. Thus, we further investigated the effect of NK on LPS-induced ROS generation in

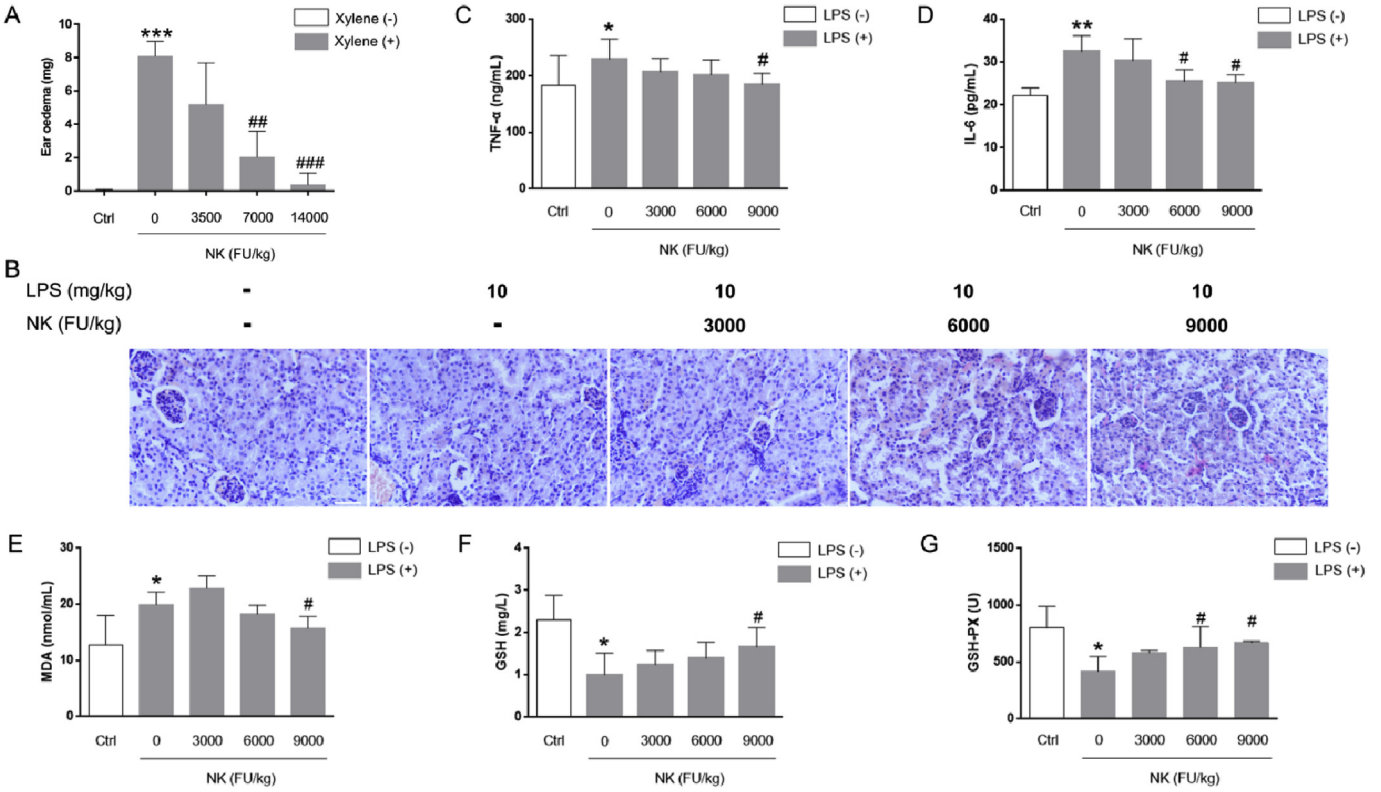


**Fig. 1. NK decreased xylene-induced ear oedema and protected against LPS-induced AKI in mice**. (A) Effects of NK on xylene-induced ear oedema in mice. Ear oedema was caused by xylene. Mice were predosed with NK (3500, 7000, and 14000 FU/kg, i.g.) for 1 week before stimulated with xylene (30 μl) on the right ear for 30 min. The ear weight was measured as described in the method section. Values were expressed as means ± SD. ***P < 0.001 vs. control; $^{\#\#}$P < 0.01, $^{\#\#\#}$P < 0.001, vs. xylene group (n = 6). (B) Effect of NK on LPS-induced AKI in mice. Mice were predosed with vehicle or NK (3000, 6000, and 9000 FU/kg, i.p.) for 1 h before LPS (10 mg/kg, i.p.) stimulation for 12 h. Kidney tissues were sectioned and stained with H&E for histopathological examination. Alternatively, blood samples were collected, and TNF-α (C) and IL-6 (D) in serum was determined using ELISA kits. Values were expressed as means ± SD. *P < 0.05, **P < 0.01 vs. control group; $^{\#}$P < 0.05 vs. LPS group. (E) Effect of NK on the MDA, GSH, and GSH-px levels in LPS-induced AKI in mice. MDA content (E), GSH levels (F), and GSH-px content (G) in serum were determined using the individual assay kits. Values were expressed as means ± SD. *P < 0.05, vs. control group; $^{\#}$P < 0.05 vs. LPS group (n = 10).

macrophage cells. As depicted in Fig. 4A, LPS exposure notably increased the intracellular level of ROS; however, pretreatment with NK (0.08, 0.15, and 0.30 FU/mL) significantly abolished this accumulation in a concentration-dependent manner, which corroborated well with our in vivo studies (Fig. 1E-G). In line with this notion, Nrf2, a master cellular sensor of oxidative stress [28], was correspondingly upregulated in exposure to LPS, which was similarly inhibited by NK concentration-dependently (Fig. 3B). In the meanwhile, AKT, a pivotal signaling bridge between ROS and NF-κB, was also activated in response to LPS treatment, which was dramatically abolished by NK in macrophage cells (Fig. 3B).

In fact, NADPH oxidase (NOX-2/gp91phox) is a major source of ROS and oxidative stress in macrophages [29]. Concordant with this scenario, it was observed that LPS promoted rapid translocation of p47phox from the cytosol to the membrane (Fig. 4C), where they assembled into an active complex that generated ROS (Fig. 4A). Interestingly, NK pretreatment remarkably suppressed the LPS-induced NOX2 activation (Fig. 4C), delineating at least in part, the underlying mechanism by which NK abolished LPS-induced ROS production in RAW264.7 macrophage cells. Collectively, these data supported the protective effect of NK against LPS-induced oxidative stress in macrophage cells.

### *3.5. NK diminished LPS-induced TLR4 activation probably via promoting TRL4 proteolysis in RAW264.7 cells*

Indeed, together with NOX2, TLR4 signaling is essential for NF-κB activation and ROS generation in macrophages [27,30]. In particular, TLR4 is the critical signaling receptor for LPS that mediates inflammatory response as well as innate and acquired immunity. Upon LPS stimulation, it dimerizes and TRAF6 is recruited, the IRAK1-TRAF6 complex phosphorylates TAB2/TAB3 and TAK1, and thus activates NF-κB and MAPKs, leading to a pathogen-specific innate immune response by releasing pro-inflammatory cytokines [31]. As such, it was observed that LPS significantly enhanced TLR4 and TRAF6 levels, which was markedly suppressed by NK in a concentration-dependent pattern (Fig. 5A). In terms of MAPKs signaling, it was found that LPS significantly activated MAPKs as reflected by the enhanced levels of p-JNK1/2, p-ERK1/2, and p-p38 in RAW264.7 cells, which were dose-dependently restrained by NK treatment (Fig. 5A). Collectively, these data suggested that NK effectively diminished LPS-induced TRL4 activation in RAW264.7 cells.

Considering the serine protease activity of NK [12], we further explored whether it would promote TLR4 proteolysis in macrophage cells. Interestingly, NK incubation mediated a time-dependent decrease in TLR4 levels in RAW264.7 macrophages (Fig. 5B). Of note, PMSF (a potent serine protease inhibitor) significantly reversed the NK-induced TLR4 proteolysis in a concentration-dependent manner (Fig. 5B), suggesting that NK promoted TLR4 degradation via its serine protease activity. Moreover, molecular docking was performed to elucidate the interaction modes between NK and TLR4. In brief, totally 100 protein-protein docking data were obtained from Hawkdock website, and the top 10 complexes of TLR4 and NK were further analyzed. Table S1 (in the supplementary data) listed their binding free energies calculated by

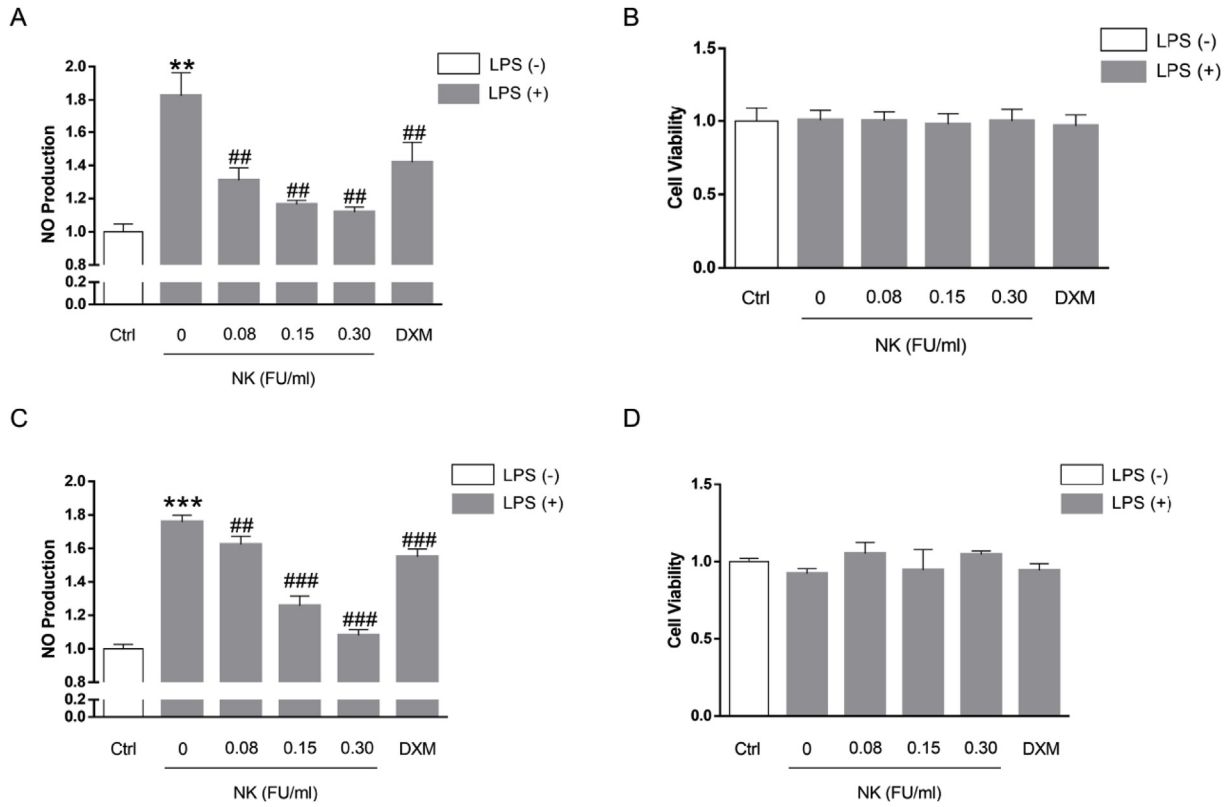


**Fig. 2. NK inhibited LPS-induced NO release in both RAW264.7 and rat primary peritoneal macrophage cells.** (A) Effect of NK on LPS-induced NO production in RAW264.7 cells. Cells were incubated with indicated concentrations of NK or dexamethasone (2 μM) for 1 h before LPS (0.1 μg/ml) stimulation for 24 h. Then, the medium was collected to determine nitrite levels using the Griess assay. (B) Effect of NK on the cell viability of RAW264.7 cells. Cell viability was determined with MTT assay. (C) Effect of NK on LPS-induced NO production in rat primary peritoneal macrophage. Cells were incubated with indicated concentrations of NK or dexamethasone (2 μM) for 1 h before LPS (0.1 μg/ml) stimulation for 24 h. Then, the medium was collected to determine nitrite levels using the Griess assay. (D) Effect of NK on the cell viability of rat primary peritoneal macrophages. Cell viability was determined with MTT assay. Data represent mean ± SD from three independent experiments. $^{**}p < 0.01$, $^{***}p < 0.001$, vs. control; $^{\#\#}p < 0.01$, $^{\#\#\#}p < 0.001$, vs. LPS-stimulated cells.

MM-GBSA algorithm as well as the non-bond interaction information. Furthermore, their binding modes and the corresponding decompositions of binding free energy were analyzed as presented in Figs. S1–S10 in the supplementary material. After a comprehensive consideration of the binding free energy and the reported catalytic site of NK, model 3 was selected for further evaluation (Fig. 6A). In brief, there were four types of non-bond inter-protein interactions among the binding surface of the two proteins, including electrostatic interactions, hydrogen bond interactions, non-classical hydrogen bond interactions, and hydrophobic interaction (Fig. 6B). Indeed, these participated residues of NK, such as Thr133, Ser105, and Ser 130, corroborated well with the reported key substrate-binding residues of NK [32] (Fig. 6B). Moreover, the binding free energy for the NK-TLR4 complex was −18.9 kcal/mol, with Van deer Waals contributed most to the structural stability of the complex (Fig. 6C). In particular, the crucial residues involved in the complex formation lay in Arg60, Tyr157, Phe36, Glu108, Thr83, Asp238, Gln185, and Asn241 of NK, and Thr255, Arg249, Lys12, Gln185 Ser183, Asn184 and Thr240 of TLR4 (Fig. 6C). In addition, the stability of the complex was validated through MD simulations. As revealed in Fig. 6D, the complex readily reached equilibration within 30 ns, and was well retained till 100 ns at least, confirming that NK and TLR4 formed a relatively stable complex, which would facilitate TLR4 proteolysis in RAW264.7 macrophages. Collectively, these combined data demonstrated that NK diminished LPS-induced TLR4 activation likely due to promoting TLR4 proteolysis in RAW264.7 macrophages. Indeed, this finding corroborated well with the Nrf2 data that NK effectively inhibited LPS-induced Nrf2 activation in RAW264.7 cells (Fig. 4B), in that, NK directly promoted TLR4 degradation (Fig. 5) as well as remarkably suppressed NOX2 activation in RAW264.7 cells (Fig. 4), thereby reducing the LPS-induced ROS generation and the corresponding Nrf2 activation.

### 3.6. NK suppressed LPS-enhanced macrophage migration and phagocytosis

Migration to pathogens and sites of inflammation is essential for macrophage cells to fulfill most of their immune/inflammatory effects. To further test the effect of NK on macrophage migration, wound healing assay was performed [33]. As shown in Fig. 7A, NK significantly inhibited their migration in a concentration-dependent manner. Moreover, phagocytosis assay was conducted to elucidate the effect of NK on phagocytic activity of macrophage cells. As illustrated in Fig. 7B, LPS significantly enhanced the phagocytosis ability of macrophage, which was abrogated by NK in a concentration-dependent pattern. These data suggested that NK suppressed the LPS-enhanced macrophage migration and phagocytosis, which confirmed the anti-inflammatory efficacy of NK in macrophage cells from the function point of view.

### 3.7. NK effectively protected against LPS-induced glomerular thrombus in mice

Mounting evidence have supported the intense crosstalk between inflammation, oxidative stress, and coagulation; Concordant with this scenario, LPS profoundly alters the fibrinolytic system of both humans and experimental animals, frequently leading to a procoagulant state and is characterized histologically by microvascular fibrin deposition in several organs, among which kidney is more likely than other organs to get injured by fibrin deposition due to its highly vascular nature [21,34]. In this regard, we further investigated the effect of NK on LPS-

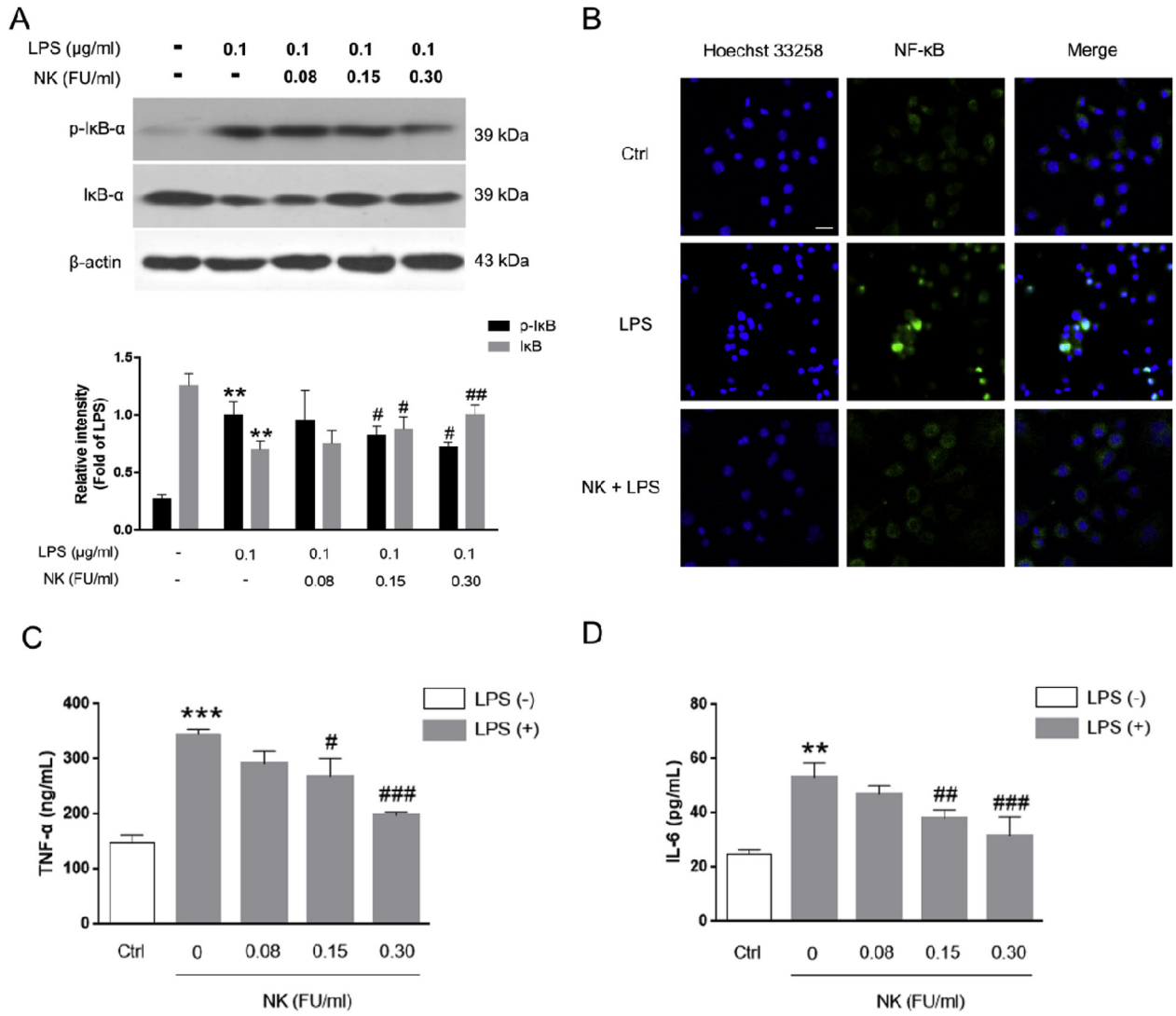


**Fig. 3. NK inhibited LPS-induced NF-κB activation in RAW264.7 cells**. (A) Effect of NK on LPS-induced IκBα activation in RAW264.7 cells. Cells were pretreated with NK (0.08, 0.15, and 0.30 FU/mL) for 1 h before being exposed to LPS (0.1 μg/ml) for 6 h. Equal amounts of total cell lysates were loaded and subjected to immunoblot analysis. β-actin was used as the control for equal protein loading and protein integrity. $^{**}P < 0.01$, vs. Control; $^{\#}P < 0.05$, $^{\#\#}P < 0.01$, vs. LPS-stimulated cells. (B) Effect of NK on LPS-induced P65 nuclear-translation in RAW264.7 cells. Cells were pretreated with NK (0.30 FU/mL) for 1 h and then exposed to LPS (0.1 μg/mL) for 6 h. Immunofluorescence analysis was performed. P65 protein was marked with green fluorescent, and the nucleus were dyed blue with Hochest. Scale bar: 40 μm. (C) Effect of NK on LPS-induced TNF-α release in RAW264.7 cells. Cells were pretreated with NK (0.08, 0.15, 0.30 FU/mL) for 1 h before LPS (0.1 μg/mL) stimulation for 24 h. Cell supernatant was collected to detect TNF-α level by ELISA. (D) Effect of NK on LPS-induced IL-6 release in RAW264.7 cells. Cells were pretreated with NK (0.08, 0.15, 0.30 FU/mL) for 1 h before LPS (0.1 μg/mL) stimulation for 24 h. Cell supernatant was collected to detect IL-6 level by ELISA. $^{**}p < 0.01$, $^{***}p < 0.001$, vs. control; $^{\#}p < 0.05$, $^{\#\#}p < 0.01$, $^{\#\#\#}p < 0.001$, vs. LPS-stimulated cells. (For interpretation of the references to colour in this figure legend, the reader is referred to the Web version of this article.)

induced glomeruli thrombus formation in mice in view of the impressive anti-inflammatory and anti-oxidative stress efficacy of NK [35–38]. As depicted by immunohistochemistry evaluations, LPS induced marked deposition of fibrin in the glomeruli of treated animals (Fig. 8A) a leading cause of acute renal failure, which lend support to a critical role of inflammation in thrombus formation. Of note, NK (6000 FU/kg and 9000FU/kg, i.p.) significantly inhibited the deposition of fibrin in the glomeruli of endotoxin-treated animals in a dose-dependent pattern as depicted by the red arrow in Fig. 8A. Indeed, LPS and/or oxidative stress caused an enhancing level of plasminogen activation inhibitor 1 (PAI-1), the main physiological inhibitor of fibrinolysis [39], thereby blocking fibrinolysis and subsequently resulting in thrombus [4]. In line with this notion, PAI-1 levels were significantly elevated in LPS-treated animals compared to those of control animals (Fig. 8B), though no effect on t-PA levels was observed (Fig. 8C). Specifically, NK administration in three different doses significantly decreased the serum concentration of PAI-1 (Fig. 8B), reinforcing PAI-1 to be an important connector between inflammation and thrombosis. Similar results were found in macrophage cells, in that LPS triggered an elevated production of PAI-1, which was significantly abrogated by NK treatment (Fig. 8D) without affecting t-PA levels (Fig. 8E). In this respect, the macrophage-derived PAI-1 may be a causative link between inflammation, oxidative stress and thrombosis, which can disrupt the fibrinolytic balance, thereby inhibiting the fibrolytic activity and triggering fibrin deposition in the glomeruli. Fascinantly, NK effectively suppressed the PAI-1 levels induced by LPS, which may underlie, at least in part, the mechanism by which NK protected against LPS-mediated thrombosis formation in mice.

## 4. Discussion

There is an evolutionary origin for the close association of

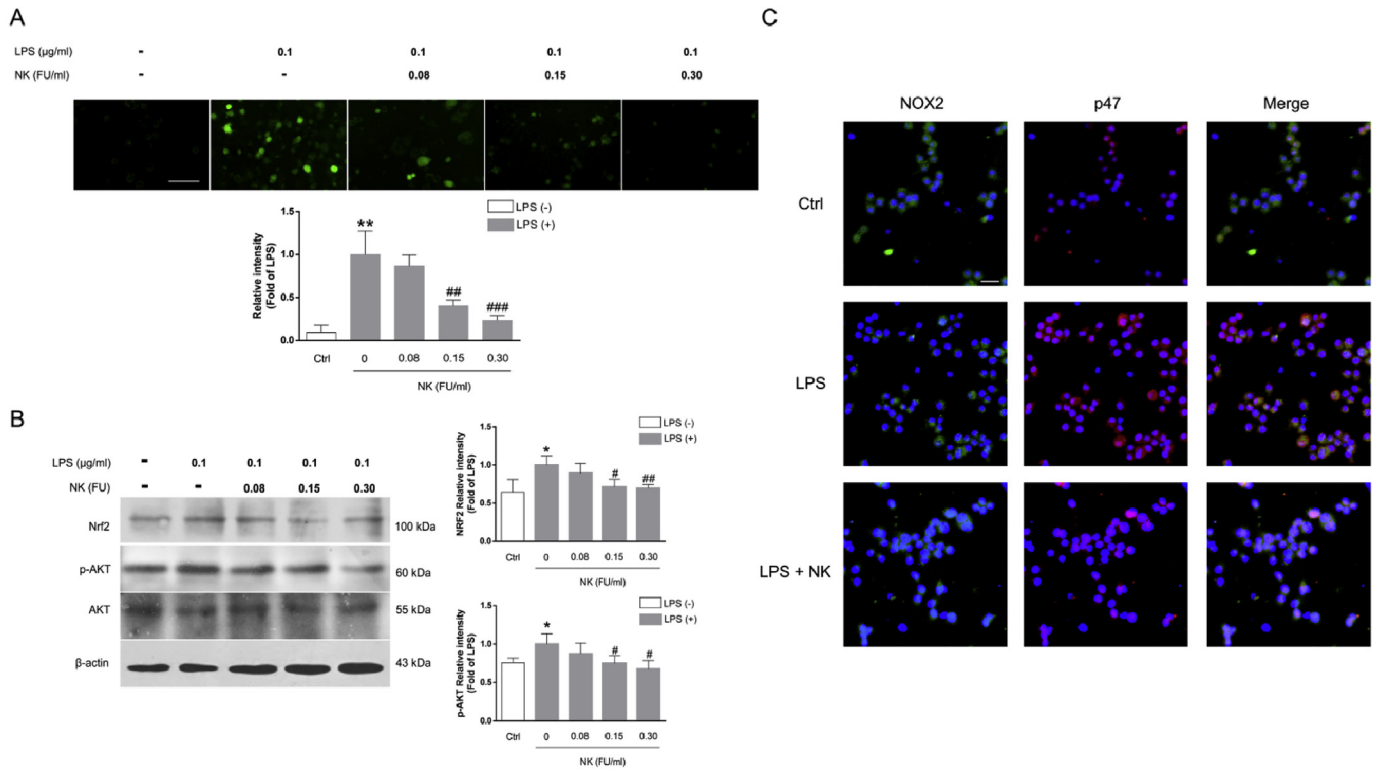


**Fig. 4. NK suppressed the LPS-induced ROS generation and NOX2 activation in RAW264.7 cells**. (A) Effect of NK on LPS-induced ROS generation in RAW 264.7 cells. Cells were pretreated with NK (0.30 FU/ml) for 1 h and then exposed to LPS (0.1 μg/mL) for 24 h. Intracellular ROS appeared green under a confocal microscopy (Scale bar is 40 μm), and the green fluorescent intensity was quantified by Image Pro Plus. Data represent the mean ± SD from three independent experiments. The mean fluorescence intensity were standardized to LPS treatment cells. $^{**}P < 0.01$, vs. control; $^{\#\#}P < 0.01$, $^{\#\#\#}P < 0.001$, vs. LPS-stimulated cells. (B) Effect of NK on LPS-induced Nrf2 and AKT activation in RAW264.7 cells. Cells were pretreated with NK (0.08, 0.15, 0.30 FU/mL) for 1 h and then were stimulated with LPS (0.1 μg/mL) for 6 h. Equal amounts of total cell lysates were loaded and subjected to immunoblot analysis. β-actin was used as the control for equal protein loading and protein integrity. Data represent the mean ± SD from three independent experiments. $^{*}P < 0.01$, vs. control; $^{\#}P < 0.05$, $^{\#\#}P < 0.05$, vs. LPS-stimulated cells. (C) Effect of NK on LPS-induced P47 translocation via immunofluorescence assay. Cells were pretreated with NK (0.30 FU/ml) for 1 h before LPS (0.1 μg/mL) stimulation for 2 h. Double immunostainings were performed with anti-NOX2 (in green) and anti-p47phox (in red); nuclei were stained with Hochest (blue). Scale bars: 40 μm. (For interpretation of the references to colour in this figure legend, the reader is referred to the Web version of this article.)

inflammation and coagulation, as injuries require both an efficient blood clotting and an inflammatory immune response against invading pathogens; however, an exaggerated response, such as acute inflammation, may shift the hemostatic balance toward a prothrombotic and antifibrinolytic state leading to potentially devastating thrombus, the key pathophysiology of CVD [40]. In light of this, many critically ill patients with a systemic inflammatory response have coagulation abnormalities [41]. And epidemiological data indicated that inflammation, as measured by C-reactive protein levels, was strongly associated with future myocardial infarction and stroke. Moreover, the reduction associated with the use of aspirin in the risk of a first myocardial infarction appeared to be directly related to the level of C-reactive protein, supporting that anti-inflammatory agents may have clinical benefits in preventing cardiovascular disease [42,43]. Along this line, we first verified the anti-inflammatory potential of NK employing the xylene-induced ear oedema model (Fig. 1A). Given that the xylene-induced activation of immunity is dependent on TLR4, and the prolonged inflammatory response can trigger systemic inflammatory conditions such as oedema and endotoxaemia [44], NK might disrupt TLR4 signaling, which was further verified by our in vitro studies in macrophage cells (Figs. 5 and 6). Moreover, the LPS-induced AKI model was employed to evaluate the impact of NK on the systemic inflammatory response. Fascinatingly, NK prominently protected against LPS-induced AKI in mice (Fig. 1B), which was accompanied by a significant inhibition of serum pro-inflammatory cytokines, such as TNF-α (Fig. 1C) and IL-6 (Fig. 1D), also a result consistent with our findings in macrophage cells (Fig. 3C and D). In the meanwhile, NK exhibited remarkable protection on LPS-induced oxidative stress as demonstrated by reversing the LPS-stimulated MDA rise and recovering LPS-induced GSH and GSH-px depletion in AKI mice (Fig. 1E-G), which again corroborated well with our in vitro studies that NK remarkably inhibited LPS-induced ROS generation in macrophage cells (Fig. 4). Accordingly, we herein provided evidence that NK exhibited promising anti-inflammatory and anti-oxidative stress efficacy.

In fact, rather than being a one-way process, thrombosis considerably promotes inflammation. For example, coagulation proteases bind to protease activated receptors (PARs) on the surface of macrophages, leukocyte, platelets, and endothelial cells, thereby propagating the thrombo-inflammatory process [45,46]. Additionally, fibrinogen and fibrin can directly stimulate expression of pro-inflammatory cytokines in mononuclear cells, endothelial cells, fibroblasts, and a variety of immune cells [47]. In particular, studies have shown interaction of fibrin with RAW 264.7 macrophage cells via TLR4, resulting in enhanced production of macrophage inflammatory protein-1alpha (MIP-1alpha), MIP-1beta, MIP-2, and monocyte chemoattractant protein-1 [48], whereas fibrinogen-deficient mice show inhibition of macrophage adhesion and less thrombin-mediated cytokine production in vivo [47]. Indeed, TLR4 on macrophages is a critical molecular link between inflammation and thrombosis via stimulating proinflammatory cytokines and PAI-1, thereby being suggested as an attractive target for antithrombotic therapy [47,49]. As a critical signaling receptor recognizing LPS, TLR4 pathway plays a pivotal role in mediating innate and acquired immunity in many cells, including macrophages [50]. When activated by LPS, TLR4 dimerizes and subsequently induces NF-κB

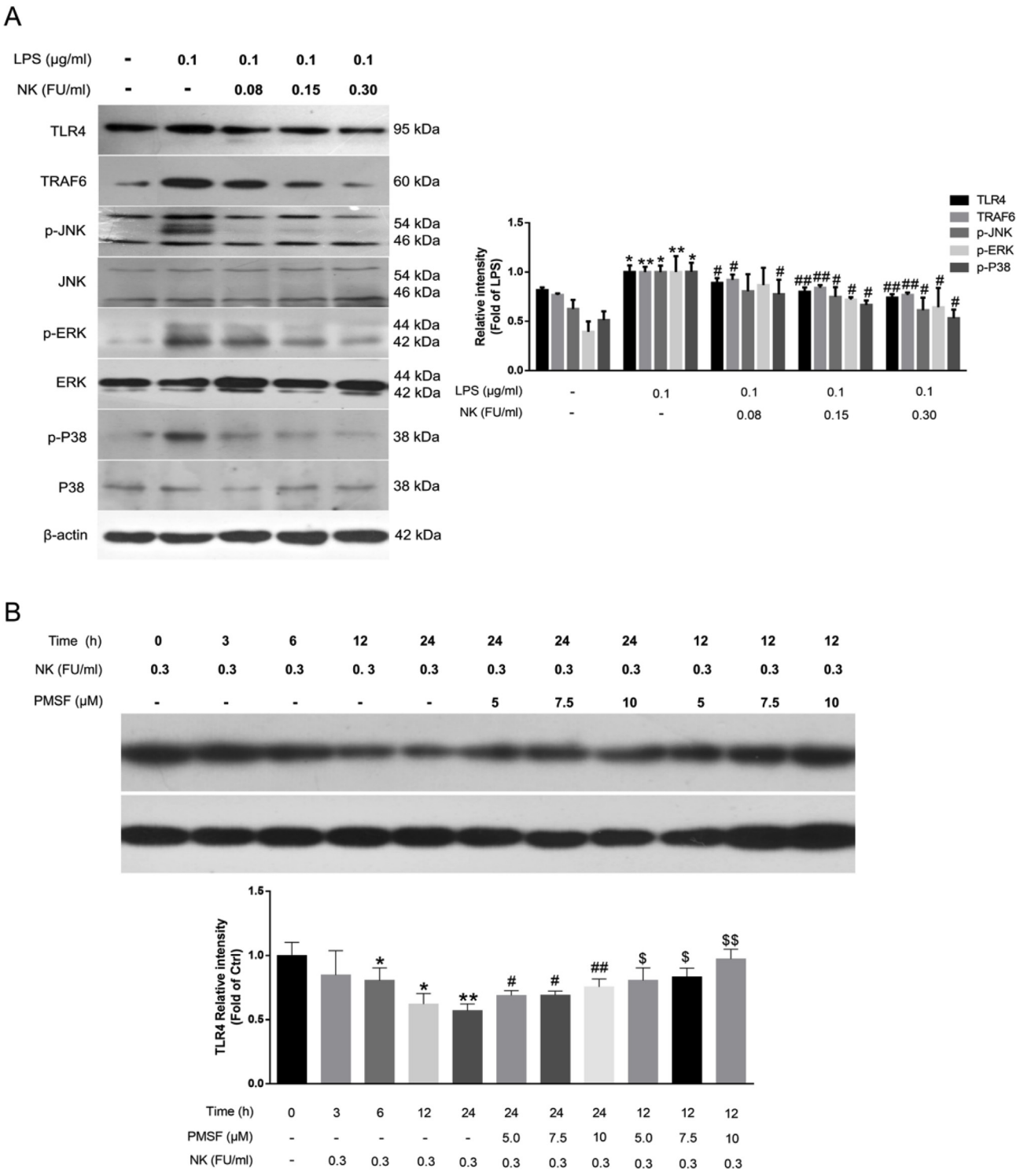


**Fig. 5. NK diminished LPS-induced TLR4 activation likely due to promoting TRL4 proteolysis in RAW264.7 cells**. (A) Effect of NK on LPS-induced TLR4 signaling pathways. Cells were pretreated with indicated concentrations of NK for 1 h and then exposed to LPS (0.1 μg/mL) for 12 h. Equal amounts of total cell lysates were loaded and subjected to immunoblot analysis. Data represent the mean ± SD from three independent experiments. (B) NK induced TRL4 degradation via its serine protease activity in RAW264.7 cells. Cells were treated with NK (0.3 FU/mL) for indicated time points with or without PMSF pretreatment for 30 min. Equal amounts of total cell lysates were loaded and subjected to immunoblot analysis. Data represent mean ± SD from three independent experiments. *P < 0.05, **P < 0.01 compared to control group; #P < 0.05, ##P < 0.05 compared to NK 12h group; $P < 0.05, $$P < 0.05 compared to NK 24h group.

translocation and MAPKs signaling transduction by interacting with its downstream bridging adaptor molecules [51]. In terms of the MyD88-dependent pathway, TRAF-6 (an actor downstream of multiple receptor families with immunoregulatory functions) facilitates TAK1 activation, which subsequently effects signaling through NF-κB and/or MAPKs pathways and eventually triggers the release of pro-inflammatory mediators [52,53]. In our study, it was revealed that NK suppressed the LPS-induced upregulation of TRAF6 (Fig. 5A), the IκB-α phosphorylation and degradation (Fig. 3A), as well as the translocation of p65 from the cytosol to the nucleus in RAW264.7 (Fig. 3B). Similarly, we noted

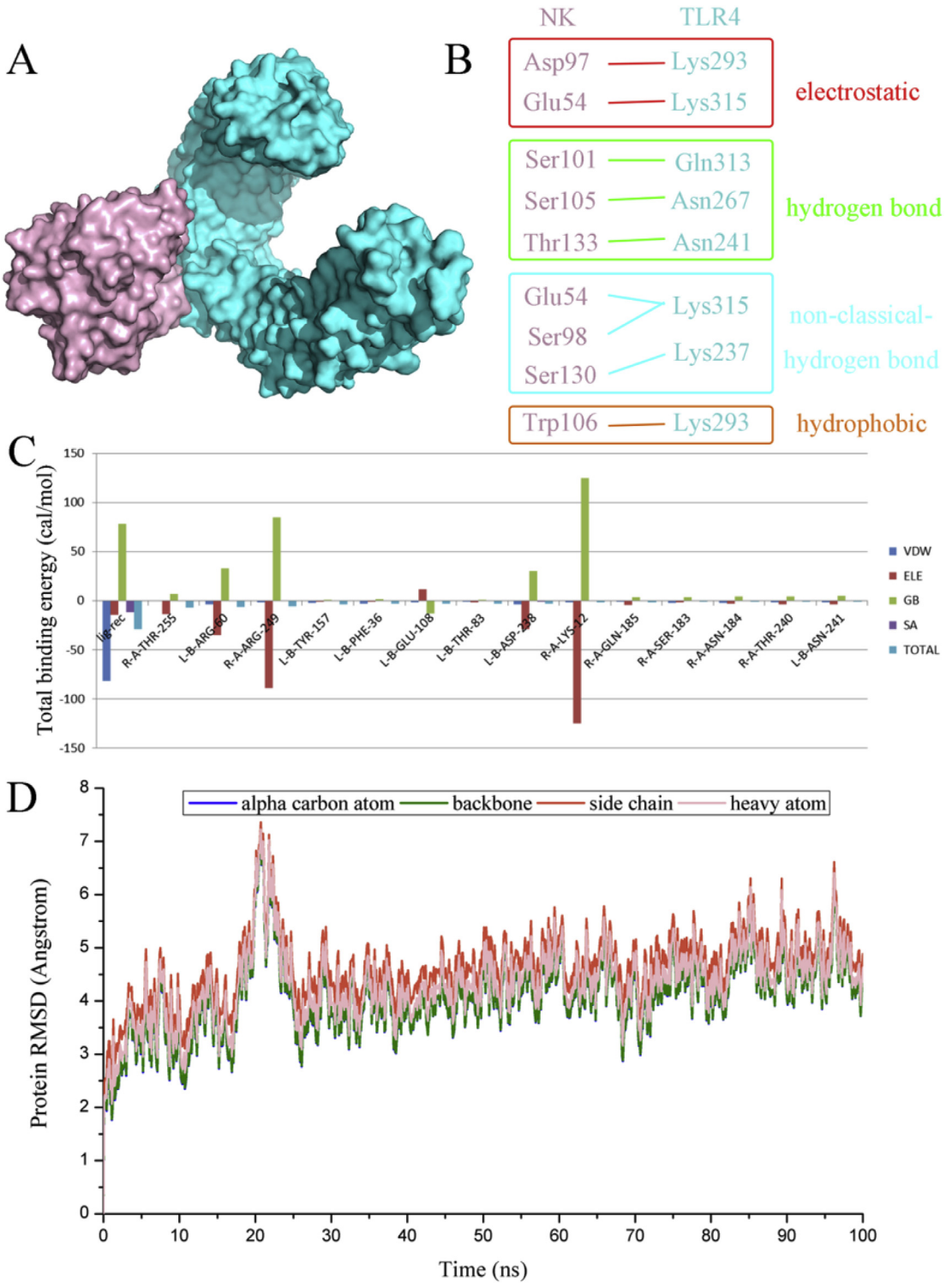


**Fig. 6. Analysis of the TLR4-NK complex selected from protein-protein docking screening**. (A) The binding mode of the protein complex. TLR4 was represented in blue and NK shown in pink. (B) The interaction types of residue pairs between TLR4 and NK were shown in details. (C) The total binding energy of the protein complex as well as the contacting residue-pairs with the total energy better than −1.0 kcal/mol calculated by MM/GBSA methods. (D) RMSD values of alpha carbon atoms, backbone atoms, side chain atoms and heavy atoms of the protein complex fluctuated along the 100 ns MD simulation. (For interpretation of the references to colour in this figure legend, the reader is referred to the Web version of this article.)

the activation of JNK1/2, ERK1/2 and p38 MAPK in the LPS-induced inflammatory process, which was inhibited by NK treatment (Fig. 5A). Along similar lines, NK was shown to repress the LPS-induced expression of inflammatory mediators, such as TNF-α, IL-6, NO, and PAI-1 in a concentration-dependent pattern (Fig. 2A and C, Fig. 3C and D, and Fig. 8D), presenting the anti-inflammatory potential of NK. Moreover, it was displayed that NK incubation time-dependently decreased TLR4 levels in macrophage cells (Fig. 5B), which was abrogated by PMSF (a potent serine protease inhibitor) in a concentration-dependent fashion (Fig. 5B). In fact, PMSF (10 μM) almost completely restored the TLR4 levels, suggesting that the serine protease activity of NK might be a major cause for decreased TLR4 expressions. In support of this

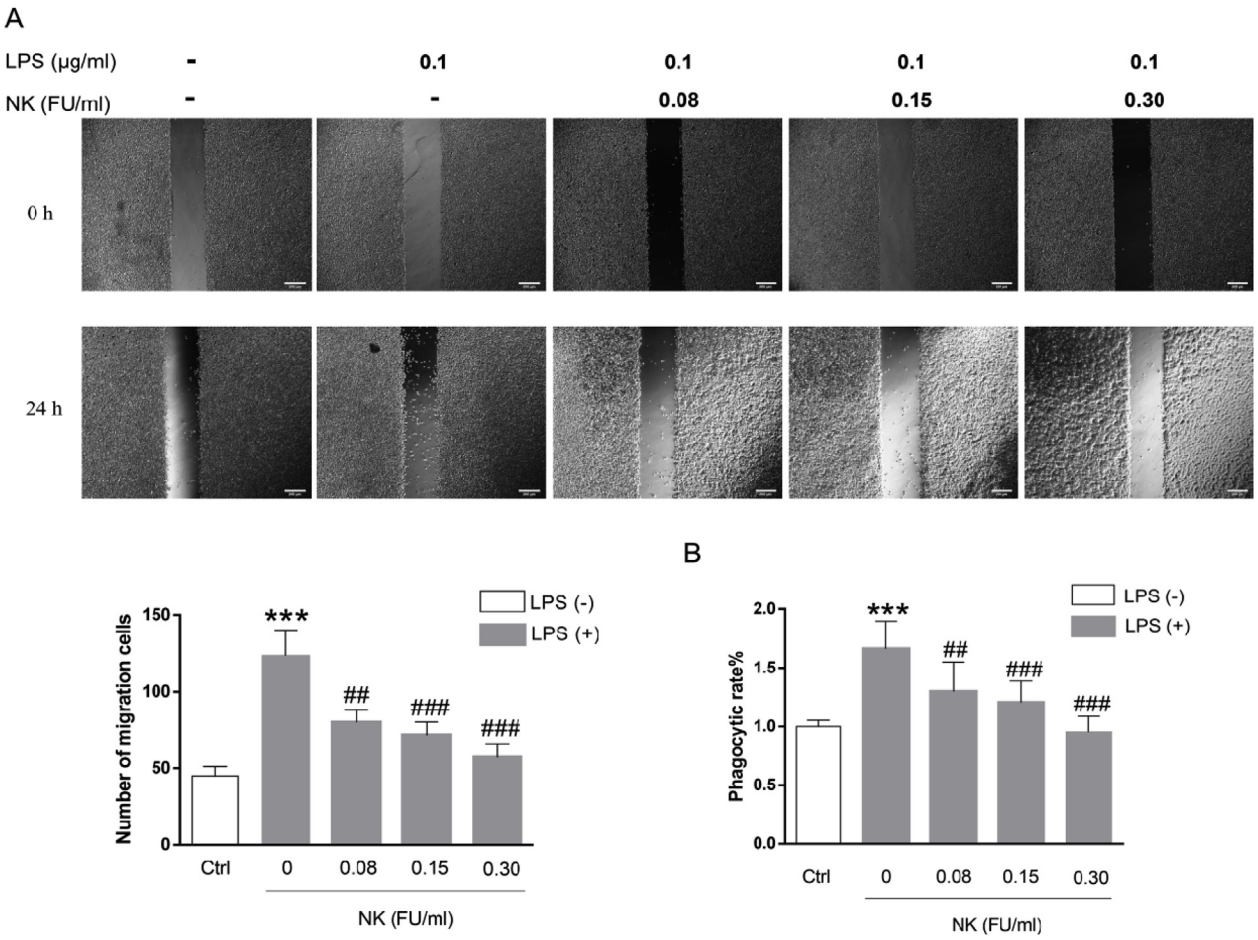


**Fig. 7. NK suppressed LPS-induced macrophage cell migration and phagocytosis**. (A) NK inhibited LPS-induced cell migration in RAW264.7 cells. Cell migration assay was performed in RAW264.7 cells treated with or without LPS (0.1 μg/mL) in the presence or absence of various concentrations of NK for 24 h. Micrographs were obtained immediately at the beginning (time 0 h) and at 24 h. The dotted lines represent the edges in the path ("wound") enclosed in time 0 h. Cells found in the path after 24 h were considered as migrating cells. Scale bar represents 200 μm. Cell counts were analyzed using ImageJ software. (B) NK inhibited LPS-induced phagocytosis in RAW264.7 cells. Cells were pretreated with NK (0.3 FU/mL) for 1 h before challenging with LPS (0.1 μg/mL) for 24 h. Then cells were incubated with neutral red for 4 h followed by extracting the phagocytic stain and measuring by microplate reader at 540 nm. Data represent the mean ± SD from three independent experiments. *p < 0.05, ***p < 0.001 vs. control; $^{\#\#}$P < 0.01, $^{\#\#\#}$P < 0.001 compared to LPS group.

interpretation, the docking and molecular simulation data further confirmed that the participated binding residues of NK overlapped with the reported key substrate-binding residues of NK, thereby facilitating the hydrolysis of TLR4 (Fig. 6).

In addition to TLR4, LPS activates NADPH oxidase abundantly expressed on macrophages, giving rise to ROS production, which potentiates macrophage activation and eventually leads to excessive inflammation [27,54]. Indeed, the main phagocytic NADPH oxidase isoform expressed in macrophages consists of two membrane bound subunits NOX2 (or gp91phox) and p22phox, the cytosolic subunits p47phox, p67phox, p40phox and a small GTPase Rac. The assembly of the active enzyme complex results in a burst of ROS production. Notably, NK was presented to remarkably inhibit the translocation of p47phox from the cytosol to the membrane in LPS-stimulated RAW264.7 cells (Fig. 4C), alleviating LPS-induced ROS generation (Fig. 4A). Indeed, chronic and acute overproduction of ROS has long been regarded as a key pathophysiological mediator that ultimately leads to CVD, since oxidative stress are associated with promoting inflammatory response, elevating platelet activation, as well as upregulating adhesion molecules (such as VWF, P-selectins, αvβ3, and ICAM-1) [64]. Moreover, NAD(P)H oxidase-dependent $O_2^{-\cdot}$ production was found in the shoulder regions of the atherosclerotic plaque, which lends the support for the role of ROS in inflammation [55]. As widely reported in literature, our data demonstrated that LPS activated both TLR4 and NOX2 abundantly expressed on the inflammatory macrophage cells, leading to the corresponding ROS production as well as the release of pro-inflammatory cytokines. In fact, in severe sepsis, circulating mononuclear cells, stimulated by these pro-inflammatory cytokines, express tissue factor, which leads to systemic activation of coagulation [56,57]. Even for healthy subjects, experimental low-dose LPS induced a 125-fold increase in tissue factor messenger RNA levels in blood monocytes [58]. To the best of our knowledge, we provided herein the first anti-inflammatory proof of NK arising from its blocking TLR4 and NOX2-mediated signaling in macrophage cells.

Of note, inflammatory process and oxidative stress are well known to impact on the fibrinolytic system to promote thrombosis [39,59]. As an important endogenous defense mechanism against thrombosis, the inhibitor of the fibrinolytic system represents a critical molecular link among fibrinolysis, inflammation, and thrombosis [59]. PAI-1 is a 50 kDa glycoprotein, the key inhibitor for fibrinolysis. It plays a major pathological role in inflammatory diseases (such as septic shock, acute lung inflammation, and thrombotic diseases), so much so that when fibrinolysis was down-regulated or inhibited by PAI-1, inflammation would exacerbate [60,61]. In fact, during LPS-induced inflammatory reaction, PAI-1 promotes inflammation through the TLR4/NF-κB pathway in vitro, while deletion of PAI-1 resulted in decreased TLR4/NF-κB pathway activity and less inflammation [60]. Moreover, there revealed the presence of a conserved distal NF-kB sites within the PAI-1

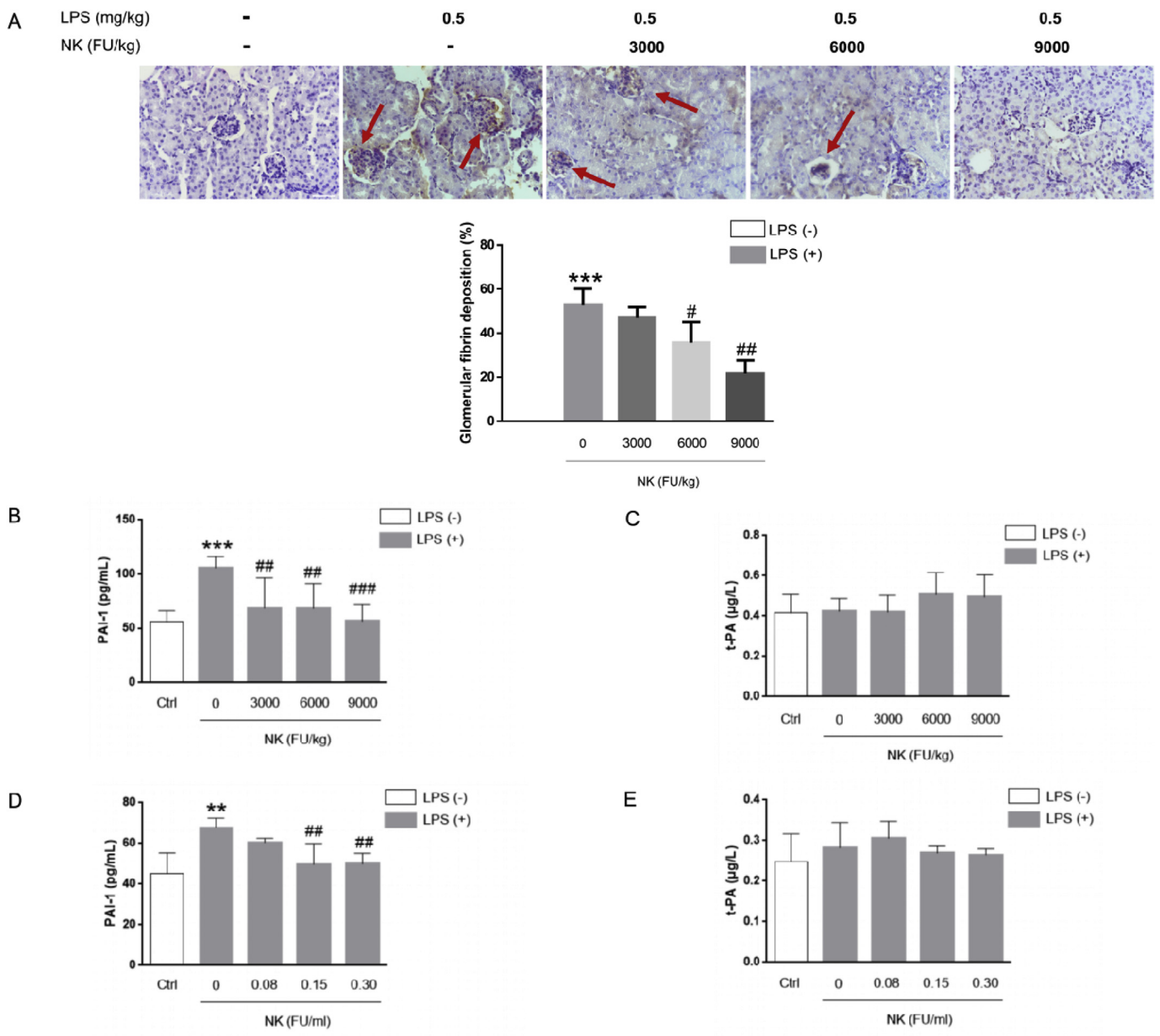


**Fig. 8. NK remarkably inhibited LPS-induced thrombosis in mice**. (A) NK inhibited LPS-induced glomerular thrombosis in mice. Mice were predosed with NK (3000, 6000, and 9000 FU/kg, i.p.) for 1 h before LPS (0.5 mg/kg, i.p.) stimulation for 12 h (n = 10). Kidney tissues were collected, and immunohistochemical staining was performed with anti-fibrin(ogen) antibody. Fibrin depositions were indicated as brown spots as indicated in red arrow, and were quantified via ImageJ. ***$p < 0.001$, vs. unstimulated group; $^{\#}p < 0.05$, $^{\#\#\#}p < 0.001$, vs. LPS group. (B) NK significantly suppressed PAI-1 release in mice. Mice were predosed with NK (3000, 6000, and 9000 FU/kg, i.p.) for 1 h LPS (0.5 mg/kg, i.p.) stimulation for 12 h. Blood was collected from mice. Serum PAI-1 (B), and t-PA (C) were determined by ELISA. ***$p < 0.001$, vs. control; $^{\#\#}p < 0.01$, $^{\#\#\#}p < 0.001$, vs. LPS group. (D) NK significantly suppressed LPS-induced PAI-1 production in RAW264.7 cells. Cells were incubated with indicated concentrations of NK for 1 h, and then stimulated with LPS (0.1 μg/mL) for 24 h. PAI-1 (D) and t-PA (E) contents were determined by ELISA. ***$p < 0.001$, vs. Control; $^{\#\#}p < 0.01$, vs. LPS-stimulated cells. (For interpretation of the references to colour in this figure legend, the reader is referred to the Web version of this article.)

promotor [62]. Accordingly, our data showed that PAI-1 was up-regulated in response to LPS stimulation in macrophage cells, which was prominently mitigated by NK, likely via TLR4/NF-kB pathways (Fig. 8D). Similarly, inflammation also promotes thrombus via up-regulation of PAI-I. For example, as previously reported, administration of LPS resulted in typical thrombus formation in glomeruli, and an elevated levels of PAI-1 in serum (Fig. 8) [21]. In the meanwhile, the importance of oxidative stress in thrombosis is highlighted by the observation that ROS up-regulate the expression level of PAI-I in endothelial cells [39], and enhanced PAI-1 expression in vasculature promotes prothrombotic phenotype and atherosclerosis in ApoE(−/−) mice [63]. In view of the vicious amplification loop between inflammation, oxidative stress and thrombosis, it is reasonable to assume that therapies inhibiting inflammation and oxidative stress might be beneficial in treating thrombus. Notably, it was revealed that NK effectively inhibited the deposition of fibrin in the glomeruli of endotoxin-treated animals in a dose-dependent manner (Fig. 8A). In particular, NK remarkably inhibited serum PAI-1 levels induced by LPS (Fig. 8B), which was consistent with our in vitro macrophage studies (Fig. 8D), highlighting the importance of the balance between prothrombotic and antithrombotic activities. Therefore, unlike the conventional interventions focusing on pharmacological thrombolytic therapy, NK holds promise as a comprehensive anti-thrombus agent, not only serving thrombolytic and anticoagulant functions, but also

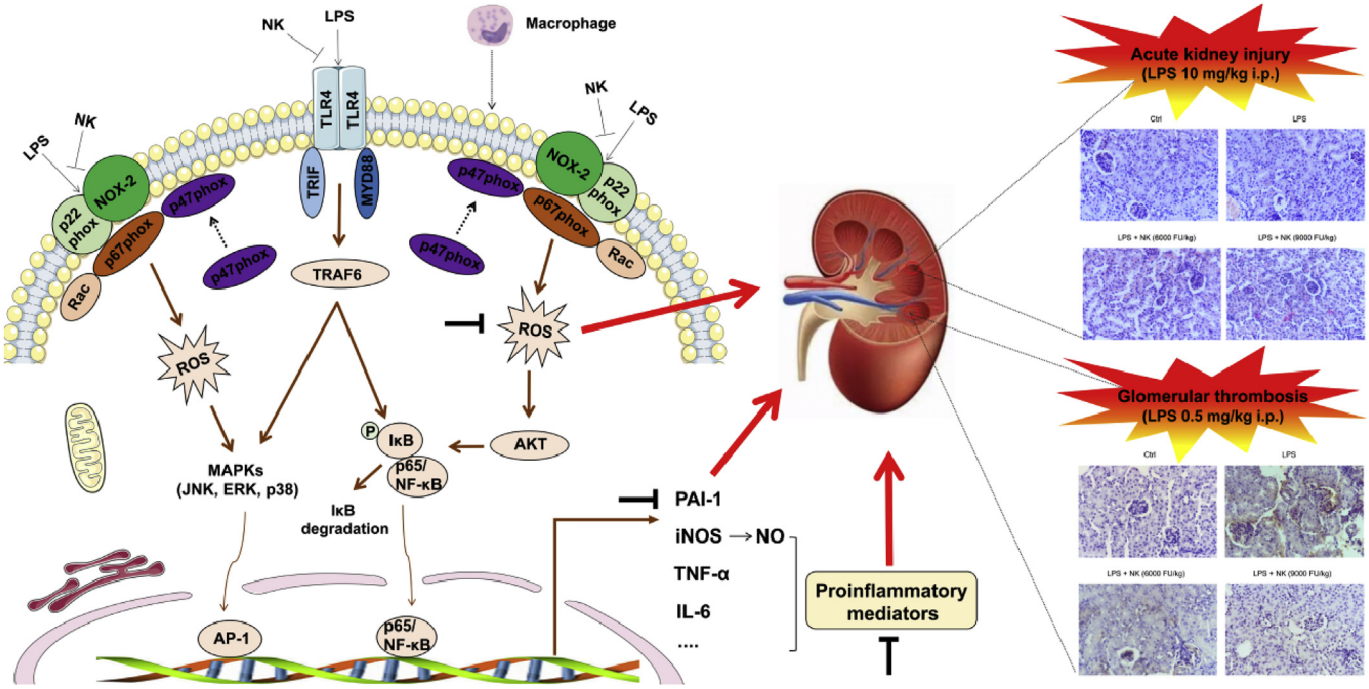


**Fig. 9. The schematic of the novel anti-thrombus insight of NK by breaking the vicious loop between inflammation, oxidative stress, and coagulation**. LPS activated both TRL4 and NOX2 abundantly expressed on the inflammatory macrophage cells, leading to the corresponding ROS production, NF-κB activation as well as its downstream pro-inflammatory mediators production, such as NO, TNF-α, IL-6, and PAI-1. Interestingly, NK remarkably suppressed LPS-induced ROS generation and NF-κB activation via inhibiting LPS-induced NOX2 and TRL4 activation, demonstrating its anti-inflammatory and anti-oxidative stress efficacy. Consistently, NK effectively protected against LPS-induced AKI in mice through restraining inflammation and oxidative stress. Of note, in support of the intense crosstalk between the inflammation, oxidative stress, and coagulation, NK effectively protected against LPS-induced glomerular thrombus in mice. In particular, PAI-1 levels, the main physiological inhibitor of fibrinolysis, were significantly elevated in LPS-treated animals, which were significantly decreased by NK treatment. Similar results were found in LPS-activated macrophages, which may underlie, at least in part, the mechanism by which NK protected against LPS-mediated thrombosis formation in mice.

eliciting anti-inflammatory and anti-oxidative stress effects that would prevent accelerated thrombosis formation (Fig. 9). From this perspective, NK may open a comprehensive anti-thrombus strategy by breaking the vicious cycle between inflammation, oxidative stress and thrombosis.

In summary, we extended the anti-thrombus mechanism of NK by demonstrating the anti-inflammatory and anti-oxidative stress effects of NK in ameliorating LPS-activated macrophage signaling and protecting against LPS-stimulated AKI as well as glomeruler thrombus in mice, opening a comprehensive anti-thrombus strategy by breaking the vicious cycle between inflammation, oxidative stress, and thrombosis.

## Declaration of competing interest

There is no conflict of interests.

## Acknowledgements

This work was supported by an award from the National Natural Science Foundation of China (21507093).

## Appendix A. Supplementary data

Supplementary data to this article can be found online at https://doi.org/10.1016/j.redox.2020.101500.

## Abbreviations

| | |
|---|---|
| NK | nattokinase |
| CVD | cardiovascular diseases |
| tPA | tissue plasminogen activator |
| LPS | lipopolysaccharides |
| TLR4 | toll-like receptor 4 |
| TNF-α | tumor necrosis factor-α |
| NO | nitric oxide |
| iNOS | inducible nitric oxide synthase |
| NF-κB | nuclear factor-κB |
| IL-6 | interleukin-6 |
| MAPK | mitogenactivated protein kinase |
| JNK | c-Jun N-terminal kinase |
| ERK | extracellular regulated protein kinases |
| MyD88 | myeloid differentiation primary response gene 88 |
| PVDF | polyvinylidene difluoride |
| ROS | reactive oxygen species |
| $DCFH_2$-DA | 2′,7′-Dichlorodihydrofluorescein diacetate |
| AKI | acute lung injury |
| H&E | hema toxylin and eosin |
| IHC | immunohistochemistry |
| MD | molecular dynamics |
| PDB | protein database bank |
| MM-GBSA | molecular mechanics-generalized Born surface area |
| SPC | simple point charge |
| RMSD | root-mean square deviations |
| PAI-1 | Plasminogen activator inhibitor-1 |

## References

[1] K. Ouriel, E.L. Welch, C.K. Shortell, K. Geary, W.M. Fiore, C. Cimino, Comparison of streptokinase, urokinase, and recombinant tissue plasminogen activator in an in vitro model of venous thrombolysis, J. Vasc. Surg. 22 (5) (1995) 593–597.
[2] J. Raffort, F. Lareyre, M. Clement, R. Hassen-Khodja, G. Chinetti, MallatZ, Monocytes and macrophages in abdominal aortic aneurysm, Nat. Rev. Cardiol. 14 (2017) 457–471.
[3] M. Levi, T. van der Poll, H.R. Büller, Bidirectional relation between inflammation

and coagulation, Circulation 109 (22) (2004) 2698–2704.
[4] S.P. Jackson, R. Darbousset, S.M. Schoenwaelder, Thromboinflammation: challenges of therapeutically targeting coagulation and other host defense mechanisms, Blood 133 (2019) 906–918.
[5] J.P. Quenot, A. Dargent, A. Large, J.B. Roudaut, P. Andreu, S. Barbar, Treatment of sepsis-induced acute kidney injury in the ICU: the therapeutic targets do not seem to be established yet, Ann. Transl. Med. 7 (2019) S181.
[6] Y. Lei, K. Wang, L. Deng, Y. Chen, E.C. Nice, C. Huang, Redox regulation of inflammation: old elements, a new story, Med. Res. Rev. 35 (2015) 306–340.
[7] G. Valen, Z.Q. Yan, G.K. Hansson, Nuclear factor kappa-B and the heart, J. Am. Coll. Cardiol. 38 (2001) 307–314.
[8] L. Edith, E.H. Diane, L. Joseph, Role of oxidative stress and nitric oxide in atherothrombosis, Front. Biosci. 13 (2008) 5323–5344.
[9] C. Nagata, K. Wada, T. Tamura, K. Konishi, Y. Goto, S. Koda, et al., Dietary soy and natto intake and cardiovascular disease mortality in Japanese adults: the Takayama study, Am. J. Clin. Nutr. 105 (2) (2017) 426–431.
[10] J.Y. Jang, T.S. Kim, J. Cai, J. Kim, Y. Kim, K. Shin, et al., Nattokinase improves blood flow by inhibiting platelet aggregation and thrombus formation, Lab. Animal Res. 29 (4) (2013) 221–225.
[11] J.Y. Kim, S.N. Gum, J.K. Paik, H.H. Lim, K.C. Kim, K. Ogasawara, et al., Effects of nattokinase on blood pressure: a randomized, controlled trial, Hypertens. Res. : Off. J. Jpn Soc. Hypertens. 31 (8) (2008) 1583–1588.
[12] H. Wu, H. Wang, F. Xu, J. Chen, L. Duan, F. Zhang, Acute toxicity and genotoxicity evaluations of nattokinase, a promising agent for cardiovascular diseases prevention, Regul. Toxicol. Pharmacol. 103 (2019) 205–209.
[13] S. Estruel-Amades, M. Massot-Cladera, P. Garcia-Cerdà, F.J. Pérez-Cano, À. Franch, M. Castell, et al., Protective effect of hesperidin on the oxidative stress induced by an exhausting exercise in intensively trained rats, Nutrients (11) (2019) (undefined.F).
[14] R. Yuan, L. Huang, L.J. Du, J.F. Feng, J. Li, Y.Y. Luo, et al., Dihydrotanshinone exhibits an anti-inflammatory effect in vitro and in vivo through blocking TLR4 dimerization, Pharmacol. Res. 142 (2019) 102–114.
[15] H.M. Berman, J. Westbrook, Z. Feng, G. Gilliland, T.N. Bhat, H. Weissig, et al., The protein data bank, Nucleic Acids Res. 28 (2000) 235–242.
[16] H.M. Kim, B.S. Park, J.I. Kim, S.E. Kim, J. Lee, S.C. Oh, et al., Crystal structure of the TLR4-MD-2 complex with bound endotoxin antagonist Eritoran, Cell 130 (2007) 906–917.
[17] J.L. Banks, H.S. Beard, Y. Cao, A.E. Cho, W. Damm, R. Farid, et al., Integrated modeling program, applied chemical theory (IMPACT), J. Comput. Chem. 26 (2005) 1752–1780.
[18] G. Weng, E. Wang, Z. Wang, H. Liu, F. Zhu, D. Li, et al., HawkDock: a web server to predict and analyze the protein-protein complex based on computational docking and MM/GBSA, Nucleic Acids Res. 47 (2019) W322–W330.
[19] M. Ylilauri, O.T. Pentikainen, MMGBSA as a tool to understand the binding affinities of filamin-peptide interactions, J. Chem. Inf. Model. 53 (2013) 2626–2633.
[20] K.J. Bowers, E. Chow, H. Xu, R.O. Dror, M.P. Eastwood, B.A. Gregersen, et al., In scalable algorithms for molecular dynamics simulations on commodity clusters, SC 2006 Conference, Proceedings of the ACM/IEEE, 2006, 2006 43-43.
[21] M.P. Tsantarliotou, S.N. Lavrentiadou, D.A. Psalla, I.E. Margaritis, M.G. Kritsepi, I.A. Zervos, et al., Suppression of plasminogen activator inhibitor-1 (PAI-1) activity by crocin ameliorates lipopolysaccharide-induced thrombosis in rats, Food Chem. Toxicol. 125 (2019) 190–197.
[22] L. Chen, S.X. Yang, E.E. Zumbrun, H.B. Guan, P.S. Nagarkatti, M. Nagarkatti, Resveratrol attenuates lipopolysaccharide-induced acute kidney injury by suppressing inflammation driven by macrophages, Mol. Nutr. Food Res. 59 (2015) 853–864.
[23] S. Sakaguchi, S. Furusawa, Oxidative stress and septic shock: metabolic aspects of oxygen-derived free radicals generated in the liver during endotoxemia, FEMS Immunol. Med. Microbiol. 47 (2) (2006) 167–177.
[24] J.D. Bailey, M. Diotallevi, T. Nicol, E. McNeill, A. Shaw, S. Chuaiphichai, et al., Nitric oxide modulates metabolic remodeling in inflammatory macrophages through TCA cycle regulation and itaconate accumulation, Cell Rep. 28 (2019) 218–230 e7.
[25] M.G. Dorrington, I.D.C. Fraser, NF-κB signaling in macrophages: dynamics, crosstalk, and signal integration, Front. Immunol. 10 (2019) 705.
[26] D.Y. Wen, Y.H. Nong, J.G. Morgan, P. Gangurde, A. Bielecki, J. DaSilva, et al., A selective small molecule I kappa B kinase beta inhibitor blocks nuclear factor kappa B-mediated inflammatory responses in human fibroblast-like synoviocytes, chondrocytes, and mast cells, J. Pharmacol. Exp. Therapeut. 317 (2006) 989–1001.
[27] W. Komatsu, H. Kishi, K. Yagasaki, S. Ohhira, Urolithin A attenuates pro-inflammatory mediator production by suppressing PI3-K/Akt/NF-κB and JNK/AP-1 signaling pathways in lipopolysaccharide-stimulated RAW264 macrophages: possible involvement of NADPH oxidase-derived reactive oxygen species, Eur. J. Pharmacol. 833 (2018) 411–424.
[28] Q. Ma, Role of nrf2 in oxidative stress and toxicity, Annu. Rev. Pharmacol. Toxicol. 53 (2013) 401–426.
[29] R.P. Brandes, N. Weissmann, K. Schröder, NOX family NADPH oxidases: molecular mechanisms of activation, Free Radic. Biol. Med. 76 (2014) 208–226.
[30] A. Singh, V. Singh, R.L. Tiwari, T. Chandra, A. Kumar, M. Dikshit, et al., The IRAK-ERK-p67phox-NOX-2 axis mediates TLR4, 2-induced ROS production for IL-1β transcription and processing in monocytes, Cell. Mol. Immunol. 13 (2016) 745–763.
[31] M.A. Saad, A.E. El-Sahhar, H.H. Arab, M.Y. Al-Shorbagy, Nicorandil abates arthritic perturbations induced by complete Freund's adjuvant in rats via conquering TLR4-MyD88-TRAF6 signaling pathway, Life Sci. 218 (2019) 284–291.
[32] S. Wu, C. Feng, J. Zhong, L. Huan, Roles of S3 site residues of nattokinase on its activity and substrate specificity, J. Biochem. 142 (3) (2007) 357–364.
[33] I. Hulkower Keren, L. Herber Renee, Cell migration and invasion assays as tools for drug discovery, Pharmaceutics 3 (2011) 107–124.
[34] K. Yamamoto, T. Shimokawa, H. Yi, K.I. Isobe, T. Kojima, D.J. Loskutoff, et al., Aging accelerates endotoxin-induced thrombosis: increased responses of plasminogen activator inhibitor-1 and lipopolysaccharide signaling with aging, Am. J. Pathol. 161 (5) (2002) 0-1814.
[35] L. Wang, J. Duan, T. Bian, R. Meng, L. Wu, Z. Zhang, et al., Inflammation is correlated with severity and outcome of cerebral venous thrombosis, J. Neuroinflammation 15 (2018) 329.
[36] J. Hirahashi, K. Hishikawa, S. Kaname, N. Tsuboi, Y. Wang, D.I. Simon, et al., Mac-1 (CD11b/CD18) links inflammation and thrombosis after glomerular injury, Circulation 120 (2009) 1255–1265.
[37] X. Yao, W. Chen, J. Liu, H. Liu, J.Y. Zhan, S. Guan, et al., Deep vein thrombosis is modulated by inflammation regulated via sirtuin 1/NF-κB signalling pathway in a rat model, Thromb. Haemostasis 119 (2019) 421–430.
[38] S.M. Day, D. Duquaine, L.V. Mundada, R.G. Menon, B.V. Khan, S. Rajagopalan, et al., Chronic iron administration increases vascular oxidative stress and accelerates arterial thrombosis, Circulation 107 (2003) 260–266.
[39] M. Swiatkowska, J. Szemraj, K.N. Al-Nedawi, Z. Pawlowska, Reactive oxygen species upregulate expression of PAI-1 in endothelial cells, Cell. Mol. Biol. Lett. 7 (2002) 1065–1071.
[40] K. Okamoto, T. Tamura, Y. Sawatsubashi, Sepsis and disseminated intravascular coagulation, J. Intensive Care 4 (2016) 23.
[41] M. Levi, S.M. Opal, Coagulation abnormalities in critically ill patients, Crit. Care 10 (2006) 222–228.
[42] B.C. Berk, W.S. Weintraub, R.W. Alexander, Elevation of C-reactive protein in "active" coronary artery disease, Am. J. Cardiol. 65 (1990) 168–172.
[43] P.M. Ridker, M. Cushman, M.J. Stampfer, R.P. Tracy, C.H. Hennekens, Inflammation, aspirin, and the risk of cardiovascular disease in apparently healthy men, N. Engl. J. Med. 336 (1997) 973–979.
[44] Y-l Liu, W-j He, L. Mo, M-f Shi, Y-y Zhu, S. Pan, et al., Antimicrobial, anti-inflammatory activities and toxicology of phenylethanoid glycosides from Monochasma savatieri Franch. ex Maxim, J. Ethnopharmacol. 149 (2013) 431–437.
[45] M.A. Cunningham, P. Romas, P. Hutchinson, S.R. Holdsworth, P.G. Tipping, Tissue factor and factor VIIa receptor/ligand interactions induce proinflammatory effects in macrophages, Blood 94 (1999) 3413–3420.
[46] S.R. Coughlin, Thrombin signalling and protease-activated receptors, Nature 407 (2000) 258–264.
[47] F.M. Szaba, S.T. Smiley, Roles for thrombin and fibrin(ogen) in cytokine/chemokine production and macrophage adhesion in vivo, Blood 99 (2002) 1053–1059.
[48] S.T. Smiley, J.A. King, W.W. Hancock, Fibrinogen stimulates macrophage chemokine secretion through toll-like receptor 4, J. Immunol. 167 (2001) 2887–2894.
[49] K. Croce, P. Libby, Intertwining of thrombosis and inflammation in atherosclerosis, Curr. Opin. Hematol. 14 (1) (2007) 55–61.
[50] F. Di Lorenzo, L. Kubik, A. Oblak, N.I. Lore, C. Cigana, R. Lanzetta, et al., Activation of human toll-like receptor 4 (TLR4)center dot myeloid differentiation factor 2 (MD-2) by hypoacylated lipopolysaccharide from a clinical isolate of Burkholderia cenocepacia, J. Biol. Chem. 290 (2015) 21305–21319.
[51] X.L. Xu, P. Yin, C.R. Wan, X.L. Chong, M.J. Liu, P. Cheng, et al., Punicalagin inhibits inflammation in LPS-induced RAW264.7 macrophages via the suppression of TLR4-mediated MAPKs and NF-kappa B activation, Inflammation 37 (2014) 956–965.
[52] Y. Yu, N.L. Ge, M. Xie, W.J. Sun, S. Burlingame, A.K. Pass, et al., Phosphorylation of Thr-178 and Thr-184 in the TAK1 T-loop is required for interleukin (IL)-1-mediated optimal NF kappa B and AP-1 activation as well as IL-6 gene expression, J. Biol. Chem. 283 (2008) 24497–24505.
[53] T. Kawai, S. Akira, Toll-like receptor downstream signaling, Arthritis Res. Ther. 7 (2005) 12–19.
[54] W.B. Zhang, F. Yang, Y. Wang, F.Z. Jiao, H.Y. Zhang, L.W. Wang, et al., Inhibition of HDAC6 attenuates LPS-induced inflammation in macrophages by regulating oxidative stress and suppressing the TLR4-MAPK/NF-κB pathways, Biomed. Pharmacother. 117 (2019) 109166.
[55] D. Sorescu, D. Weiss, B. Lassegue, R.E. Clempus, K. Szocs, G.P. Sorescu, et al., Superoxide production and expression of nox family proteins in human atherosclerosis, Circulation 105 (2002) 1429–1435.
[56] B. Osterud, L.V. Rao, J.O. Olsen, Induction of tissue factor expression in whole blood-lack of evidence for the presence of tissue factor expression on granulocytes, Thromb. Haemostasis 83 (2000) 861–867.
[57] M. Levi, T. van der Poll, H. ten Cate, S.J. van Deventer, The cytokine-mediated imbalance between coagulant and anticoagulant mechanisms in sepsis and endotoxaemia, Eur. J. Clin. Invest. 27 (1997) 3–9.
[58] R.F. Franco, E. de Jonge, P.E. Dekkers, J.J. Timmerman, C.A. Spek, S.J. van Deventer, et al., The in vivo kinetics of tissue factor messenger RNA expression during human endotoxemia: relationship with activation of coagulation, Blood 96 (2000) 554–559.
[59] R.L. Medcalf, Fibrinolysis, inflammation, and regulation of the plasminogen activating system, J. Thromb. Haemostasis (2007) 132–142 null.
[60] W. Ren, Z. Wang, F. Hua, L. Zhu, Plasminogen activator inhibitor-1 regulates LPS-induced TLR4/MD-2 pathway activation and inflammation in alveolar macrophages, Inflammation 38 (2015) 384–393.
[61] F. Hua, W. Ren, L. Zhu, Plasminogen activator inhibitor type-1 deficiency exaggerates LPS-induced acute lung injury through enhancing Toll-like receptor 4 signaling pathway, Blood Coagul. Fibrinolysis 22 (2011) 480–486.
[62] B. Hou, M. Eren, C.A. Painter, J.W. Covington, J.D. Dixon, J.A. Schoenhard, et al., Tumor necrosis factor alpha activates the human plasminogen activator inhibitor-1 gene through a distal nuclear factor kappaB site, J. Biol. Chem. 279 (2004) 18127–18136.
[63] K. Schafer, K. Muller, A. Hecke, E. Mounier, J. Goebel, D.J. Loskutoff, et al., Enhanced thrombosis in atherosclerosis-prone mice is associated with increased arterial expression of plasminogen activator inhibitor-1, Arterioscler. Thromb. Vasc. Biol. 23 (2003) 2097–2103.
[64] M. Mittal, M.R. Siddiqui, K. Tran, S.P. Reddy, A.B. Malik, Reactive oxygen species in inflammation and tissue injury, Antioxidants Redox Signal. 20 (7) (2013).